Electronic Supplementary Material (ESI) for Nanoscale.

Supporting Information

Targeting myeloid regulators by paclitaxel-loaded enzymatically degradable cups

*Seth C. Burkert,[a] Galina V. Shurin,[b] David L. White,[a] Xiaoyun He,[a] Alexandr A. Kapralov,[c] Valerian E. Kagan,[a,c,d,e,f] Michael R. Shurin,[b,g] and Alexander Star[a]**

[a]Department of Chemistry, University of Pittsburgh, Pittsburgh, Pennsylvania 15260, United States

[b]Department of Pathology, University of Pittsburgh Medical Center, Pittsburgh, Pennsylvania 15261, United States

[c]Department of Environmental and Occupational Health, University of Pittsburgh, Pittsburgh Pennsylvania, United States

[d]Department of Pharmacology and Chemical Biology, University of Pittsburgh, Pittsburgh Pennsylvania, United States

[e]Department of Radiation Oncology, University of Pittsburgh, Pittsburgh Pennsylvania, United States

[f]Laboratory of Navigational Redox Lipidomics, IM Sechenov Moscow State Medical University, Russia

[g]Department of Immunology, University of Pittsburgh Medical Center, Pittsburgh, Pennsylvania 15261, United States

*Corresponding Author Email: astar@pitt.edu

Table of Contents

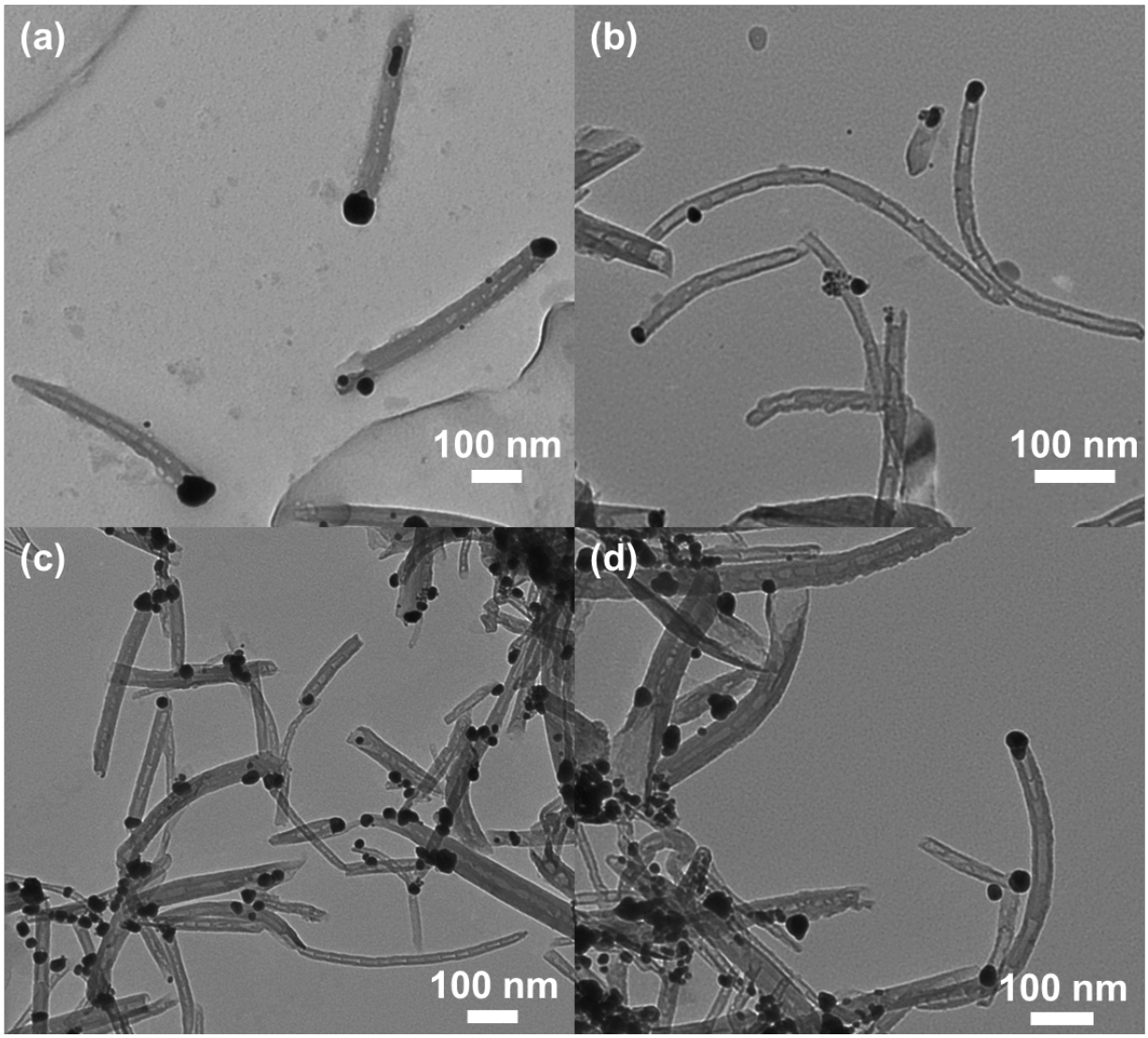

Figure S1. Representative TEM images of Au-NCNC synthesized in (a) nanopure water; (b) 1X phosphate buffer; (c) 1X phosphate buffer and ethanol; and (d) 1X phosphate buffer and paclitaxel suspended in ethanol. Observe that free gold nanoparticles are more abundant upon the addition of ethanol to the corking solution.

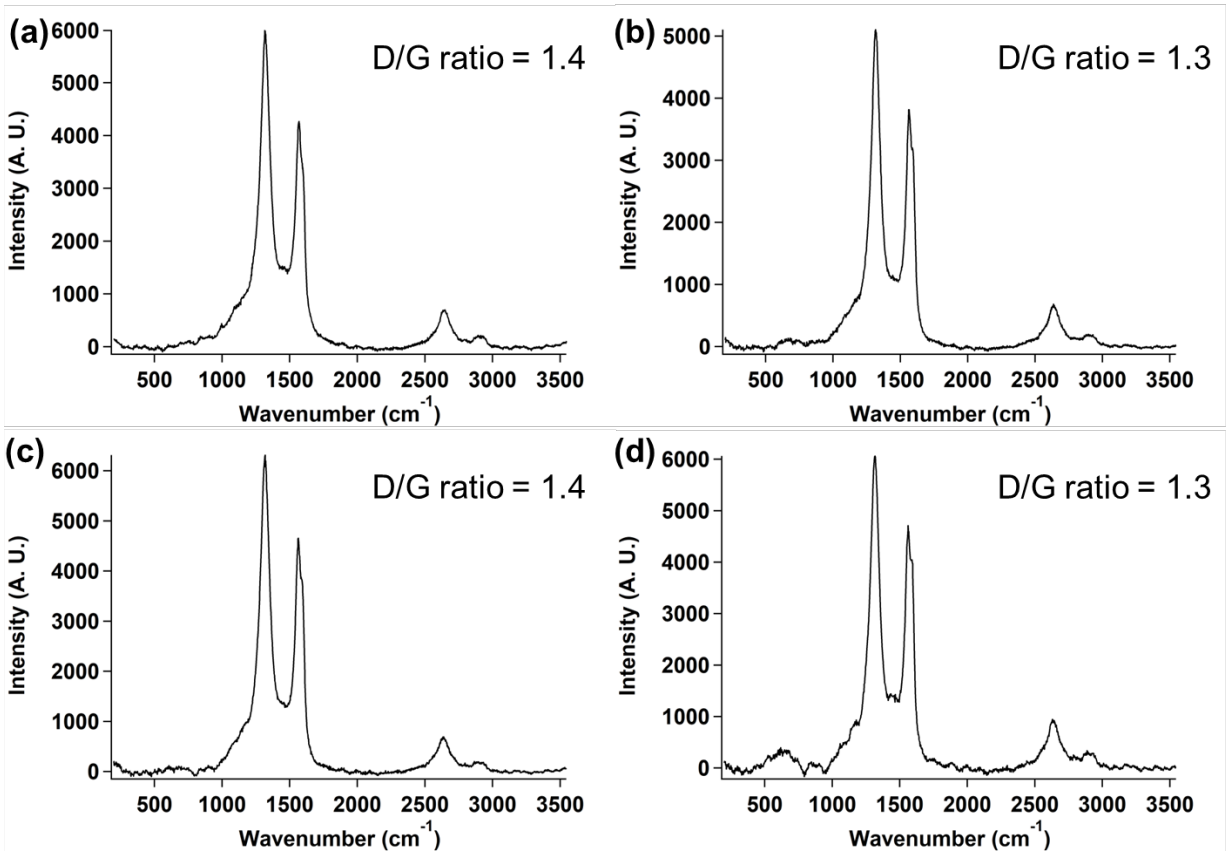

Figure S2. Raman characterization with inset D/G ratios for Au-NCNC synthesized in (a) nanopure water; (b) 1X phosphate buffer; (c) 1X phosphate buffer and ethanol; and (d) 1X phosphate buffer and paclitaxel suspended in ethanol.

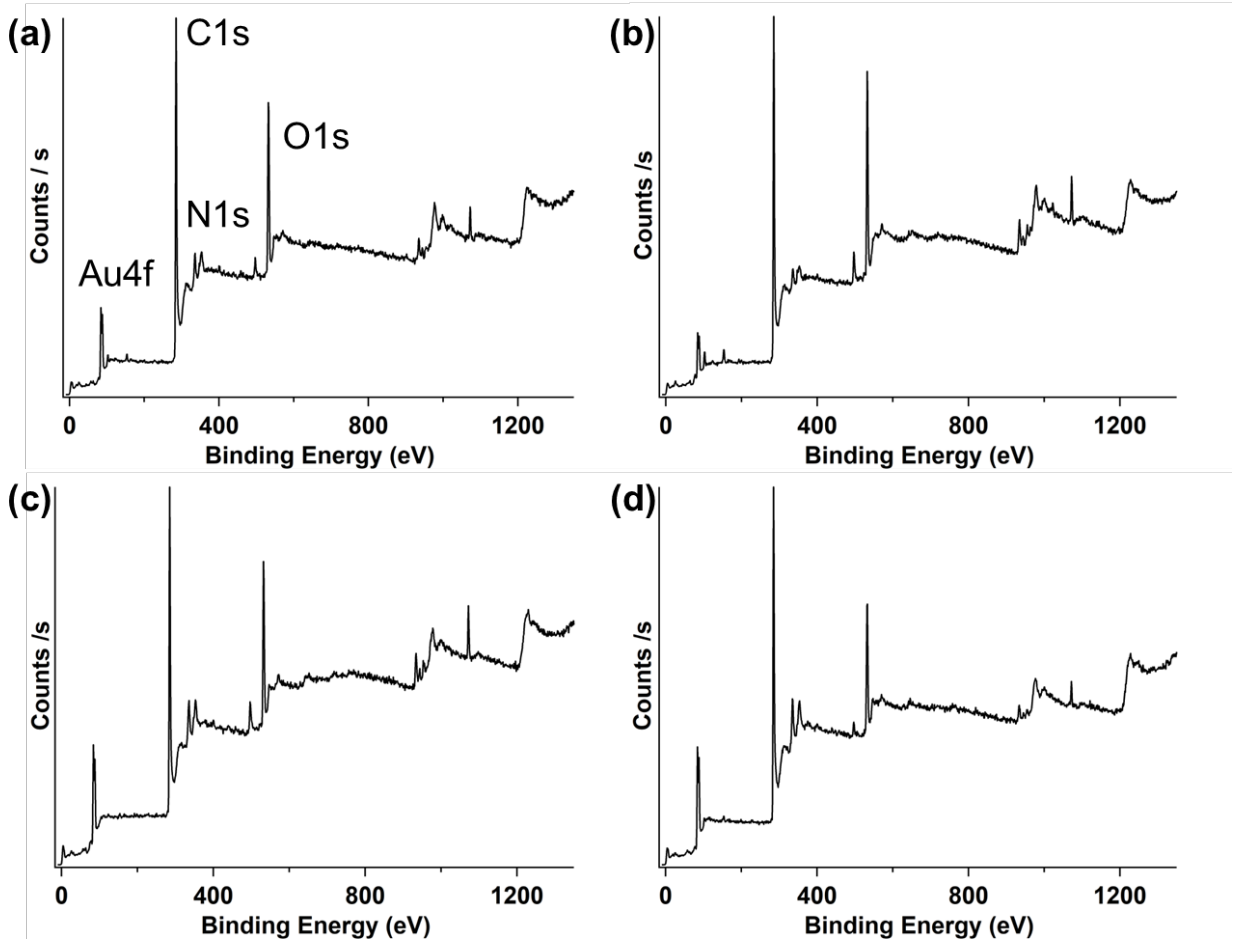

Figure S3. XPS survey characterization of Au-NCNC synthesized in (a) nanopure water; (b) 1X phosphate buffer; (c) 1X phosphate buffer and ethanol; and (d) 1X phosphate buffer and paclitaxel suspended in ethanol.

Table S1. Atomic percent of each Au-NCNC sample as determined by survey XPS

Element	Normal	Buffer	Ethanol	Taxol
C1s	79.07 %	77.54 %	79. 15 %	82.42 %
O1s	18.03 %	20.41 %	17.09 %	14.94 %
N1s	1.84 %	1.36 %	2.26 %	1.05 %
Au4f	1.06 %	0.69 %	1.50 %	1.60 %

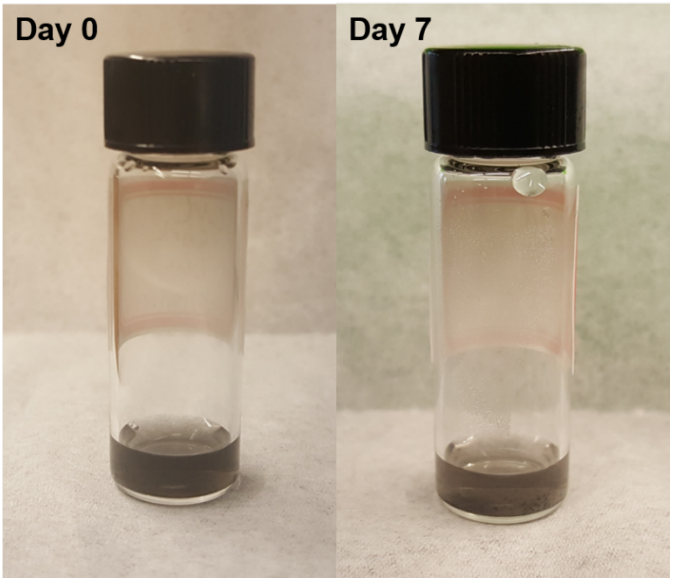

Figure S4. Photographs of paclitaxel loaded Au-NCNC on Day 0 and Day 7 illustrating colloidal stability of the particles.

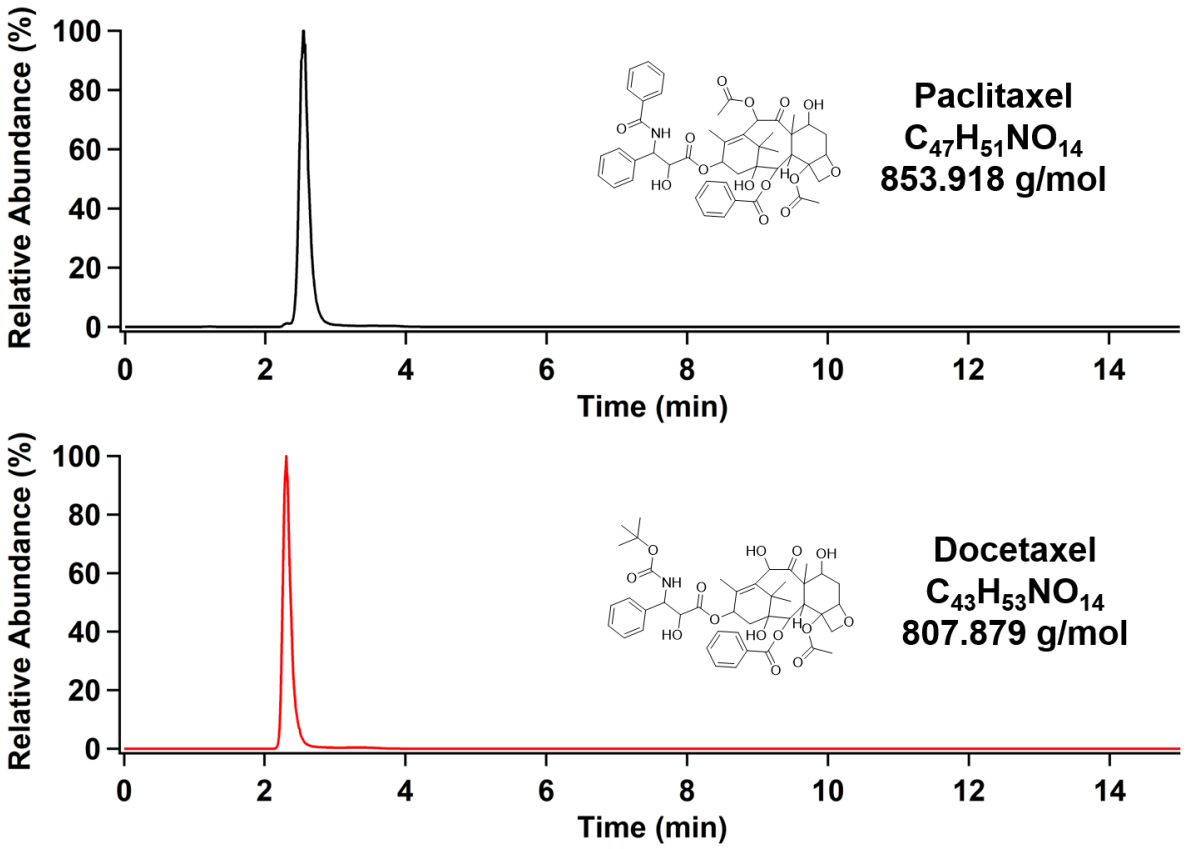

Figure S5. LC-MS chromatogram of paclitaxel and docetaxel with associated chemical structure and molecular weight.

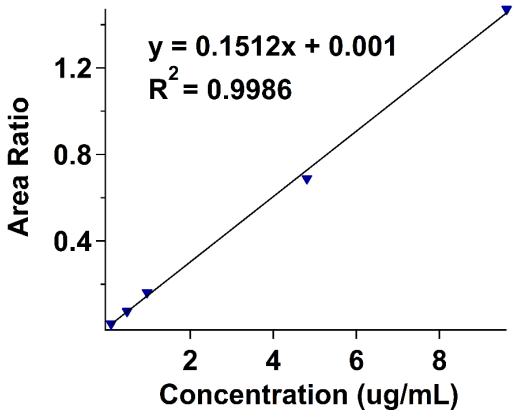

Figure S6. Calibration plot for the quantification of paclitaxel.

Table S2. Bio-distribution of gold atoms as detected by ICP-MS

	ppb Au / mg tissue		
Day 6	**B16 melanoma (control)**	**Empty Au-NCNC**	**Paclitaxel Au-NCNC**
Heart	0.005 ± 0.000	0.096 ± 0.003	0.062 ± 0.002
Liver	0.035 ± 0.000	18.260 ± 1.314	53.962 ± 1.150
Lung	0.014 ± 0.000	12.145 ± 0.141	6.384 ± 0.101
Spleen	0.033 ± 0.001	16.828 ±0.887	39.069 ± 0.645
Tumor	0.009 ± 0.001	0.316 ± 0.013	0.138 ± 0.006
Day 8	**B16 melanoma (control)**	**Empty Au-NCNC**	**Paclitaxel Au-NCNC**
Heart	0.007 ± 0.000	0.108 ± 0.001	0.145 ± 0.010
Liver	0.006 ± 0.000	81.204 ± 1.622	20.891 ± 0.363
Lung	0.010 ± 0.001	32.557 ± 0.620	0.892 ± 0.010
Spleen	0.013 ± 0.001	208.916 ± 2.561	42.387 ± 0.505
Tumor	0.006 ± 0.000	0.194 ± 0.009	0.066 ± 0.002
Day 13	**B16 melanoma (control)**	**Empty Au-NCNC**	**Paclitaxel Au-NCNC**
Heart	0.016 ± 0.008	0.055 ± 0.003	0.073 ± 0.003
Liver	0.007 ± 0.000	26.904 ± 0.134	16.118 ± 0.304
Lung	0.026 ± 0.000	63.950 ±1.102	13.910 ± 0.329
Spleen	0.025 ± 0.001	123.912 ± 3.042	75.931 ± 1.034
Tumor	0.006 ± 0.001	0.068 ± 0.001	0.067 ± 0.003

Each sample was run in triplicate with the average of the triplicate measurements being reported ± the standard deviation of the measurements. The gold ppb concentration of each data point was normalized to the mass of the tissue sample.

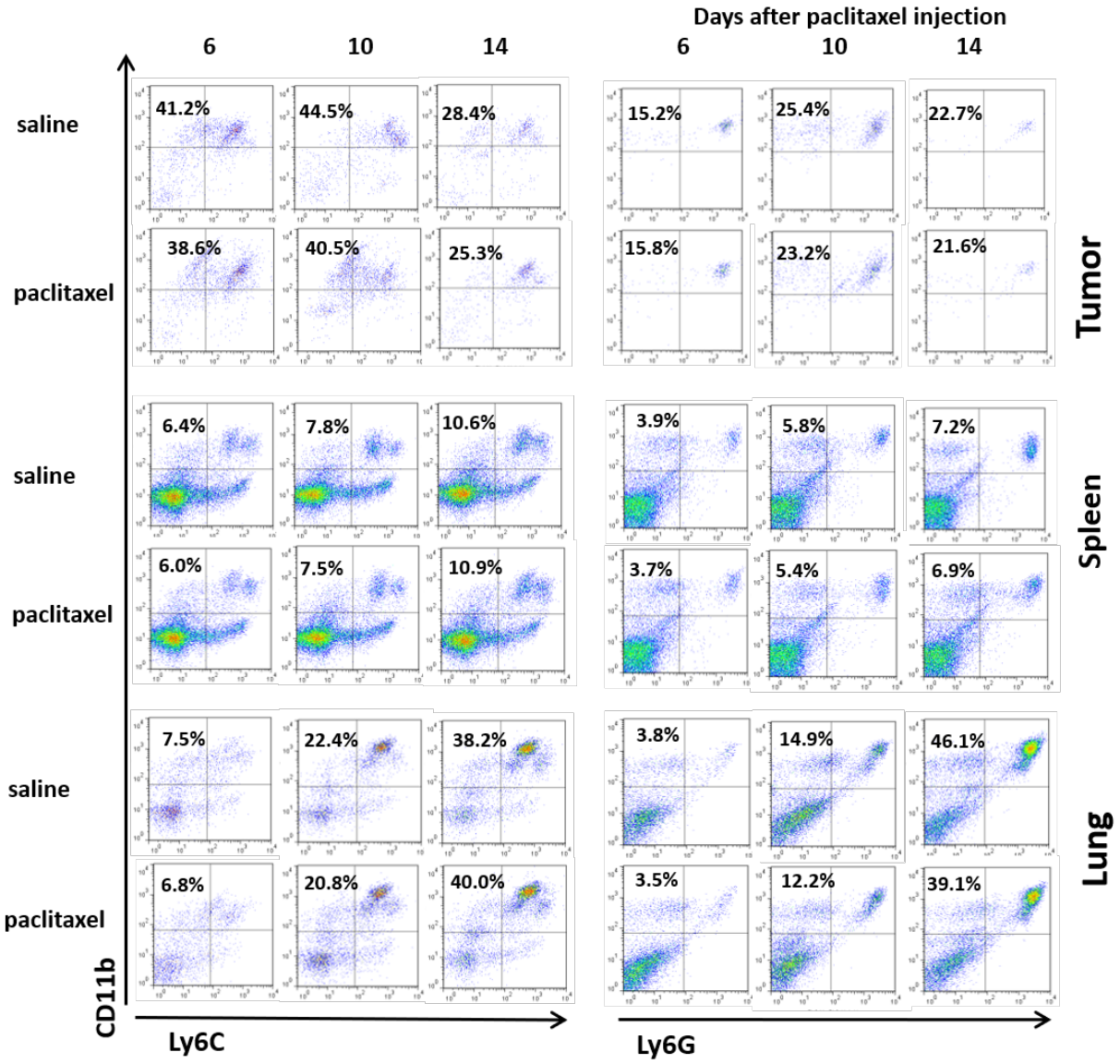

Figure S7. B16 melanoma-bearing mice were tail vein injected with saline and free paclitaxel, and tissues were harvested at different time points as shown. Tissues were digested, and single cell suspensions were prepared and stained as described in the experimental section. Representative flow cytometry results are shown for CD45 gated cell populations. The levels of monocytic CD11bLy6C^{high}Ly6G$^{low/neg}$ M-MDSC and polymorphonuclear CD11bLy6G^{high}Ly6C$^{low/neg}$ PMN-MDSC are shown. Two independent experiments revealed similar results.